International Tables for Crystallography (2006). Vol. F, Chapter 6.2, pp. 133–142.

6.2. Neutron sources

BY B. P. SCHOENBORN AND R. KNOTT

6.2.1. Reactors

The generation of neutrons by steady-state nuclear reactors is a well established technique (Bacon, 1962; Kostorz, 1979; Pynn, 1984; Carpenter & Yelon, 1986; Windsor, 1986; West, 1989). Reactor sources that play a major role in neutron-beam applications have a maximum unperturbed thermal neutron flux, $\varphi_{\rm th}$, within the range $1 < \varphi_{\rm th} < 20 \times 10^{14}$ cm^{-2} s^{-1}. A research reactor is essentially a matrix of fuel, coolant, moderator and reflector in a well defined geometry (Fig. 6.2.1.1). The fuel is uranium, and neutron-induced fission in the isotope ^{235}U produces a number of prompt and delayed neutrons (slightly more than a total of two) and, on average, one of these is required to maintain the steady-state chain reaction (*i.e.* criticality). The heat generated ($\sim$200 MeV per fission event) must be removed, hence the need for an efficient coolant. In practice, the simultaneous requirements of complex thermal hydraulics and nuclear reaction kinetics must be addressed. The neutrons produced in the fission event have a mean energy of $\sim$1 MeV, and a material is required to reduce this energy to $\sim$25 meV to take advantage of the larger fission cross section of ^{235}U in the 'thermal' energy range. Such a moderator is composed of a material rich in light nuclei, so that a large fraction of the neutron energy is transferred per collision.

There is an inherent maximum in neutron flux density imposed by the fission process (the number of excess neutrons produced per fission event), by the reduced density of neutron-generation material required for cooling purposes and by the heat-removal capacity of suitable coolants. Detailed design of reactor systems is essential to obtain the correct balance.

6.2.1.1. *Basic reactor physics*

Reactor physics is the theoretical and experimental study of the neutron distributions in the energy, spatial and time domains (Soodak, 1962; Jakeman, 1966; Akcasu *et al.*, 1971; Glasstone & Sesonske, 1994). The fundamental relation describing neutron kinetics is the Boltzmann transport equation (*e.g.* Spanier & Gelbard, 1969; Stamm'ler & Abbate, 1983; Weisman, 1983; Lewis & Miller, 1993). In theory, the transport equation describes the life of the neutron from its birth as a high-energy component of the fission process, through the various diffusion and moderation processes, until its ultimate end in (i) the chain reaction, (ii) leakage into beam tubes, or (iii) parasitic absorption (Williams, 1966). In practice, the complex nuclear reactions and the geometrical configurations of the component materials are such that a rigorous theoretical analysis is not always possible, and simplifying approximations are necessary. Nevertheless, well proven algorithms have been developed, and many have been included in computer codes (*e.g.* Hallsall, 1995).

On examination of the factors that influence the neutron flux distribution, there are three distinct but interdependent functions performed by the coolant, moderator and reflector. The coolant/moderator is of major importance in the fuelled region to sustain optimum conditions for the chain reaction, and the moderator/reflector is important in the regions surrounding the central core (Section 6.2.1.2). It should be noted that reactors for neutron-beam applications must be substantially undermoderated in order to provide a fast neutron flux at the edge of the core, which can be thermalized at the entry to the beam tubes. Most research reactors use H_2O or D_2O as the coolant/moderator.

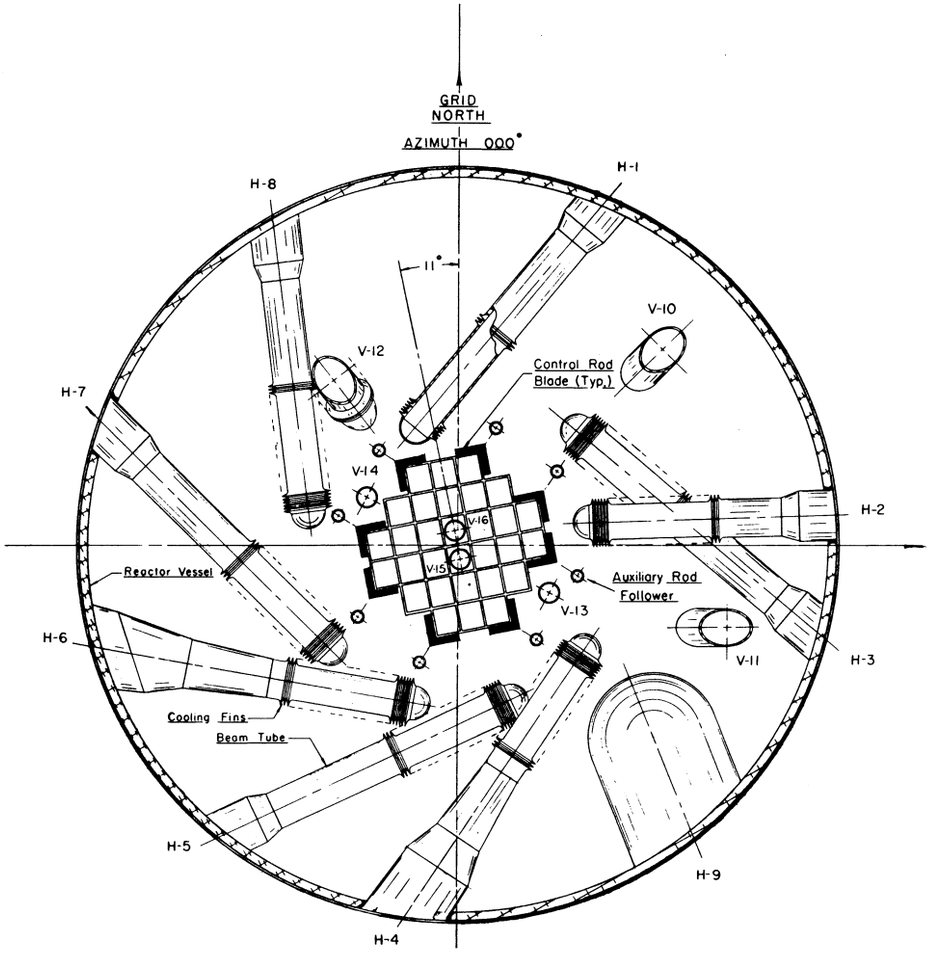

Fig. 6.2.1.1. Schematic of the High Flux Beam Reactor at the Brookhaven National Laboratory (USA). The central core region (48 cm in diameter and 58 cm high) contains 28 fuel elements in an array surrounded by an extended D_2O moderator/reflector region. The diameter of the reactor vessel is approximately 2 m. All but one of the beam tubes are tangentially oriented with respect to the core. The cold neutron source is located in the H9 beam tube.

6.2.1.2. *Moderators for neutron scattering*

The moderator/reflector serves to modify the energy distribution of fast neutrons leaking from the central core, returning a significant number of thermalized neutrons to the core region to provide for criticality with a smaller inventory of fuel and providing excess neutrons for a range of applications, including neutron-beam applications. The moderator/reflector may be H_2O, D_2O, Be, graphite or a combination of these. Almost all choices have been used; however, the optimum is not achieved with any choice, and priorities must be set in terms of neutron-beam performance, other source activities and the reactor fuel cycle.

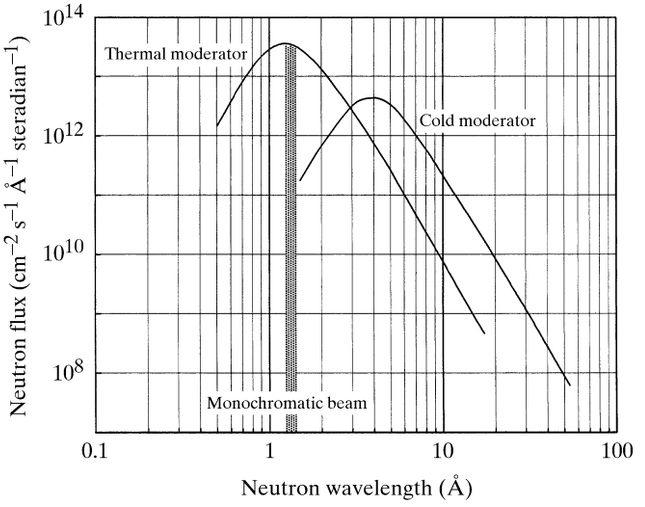

Fig. 6.2.1.2. Neutron wavelength distributions for a thermal (310 K) and a cold (30 K) neutron moderator in a 'typical' dedicated beam reactor. The Maxwellian distribution merges with a $1/E$ slowing-down distribution at shorter wavelengths. A wavelength distribution for a monochromatic beam application on a thermal source is illustrated. It should be noted that, depending on the value of the mean wavelength for the monochromatic beam, harmonic contamination may be significant.

For neutron-beam applications, D_2O is the preferred reflector material since the moderation length is large and the absorption cross section low. Consequently, the thermal neutron flux peak is rather broad and occurs relatively distant from the core. While the exact position of the peak depends on the reactor core design, the peak width has a major impact on beam-tube orientation (Section 6.2.1.3). The combination of D_2O coolant/moderator–D_2O moderator/reflector provides a distinct advantage; however, for a number of technical reasons, the H_2O–D_2O combination is becoming more common, with the D_2O in a closed vessel surrounding the central H_2O-cooled core.

6.2.1.2.1. *Thermal moderators*

Neutrons thermalized within a 'semi-infinite' moderator/reflector typical of a steady-state reactor source establish an equilibrium Maxwellian energy distribution characterized by the temperature (T) of the moderator (Fig. 6.2.1.2). The wavelength, λ_m, at which the above distribution has a maximum is given by

$$\lambda_m = h/(5k_BTm_n)^{1/2}.$$

Depending on the width of the moderator and its composition, the Maxwellian distribution merges with the $1/E$ slowing-down distribution from the reactor core to give a total distribution at the beam-tube entry.

Clearly, the neutron wavelength distribution will depend on the local equilibrium conditions. Since steady-state reactors typically operate with moderator/reflector temperatures in the range 308–323 K, the corresponding λ_m is about 1.4 Å (Fig. 6.2.1.2). However, it is possible to alter the neutron distribution by re-thermalizing the neutrons in special moderator regions, which are either cooled significantly below or heated significantly above the average moderator temperature. One such device of prime importance is the cold moderator in the form of a cold source.

6.2.1.2.2. *Cold moderators*

The thermal neutron distribution shown in Fig. 6.2.1.2 is not ideal for all experiments, since the flux of 5 Å neutrons is almost two orders of magnitude less than the peak. The solution is to introduce a cold region in the moderator/reflector. This is typically a volume of liquid H_2 or D_2 at $\sim$10–30 K, and a Maxwellian distribution around this temperature results in a λ_m of $\sim$4 Å. The geometric design of a cold-source vessel has been shown to be very important, with substantial gains in neutron flux obtained by innovative design. A re-entrant geometry approximately 20 cm in diameter filled with liquid D_2 at 10 K provides optimum neutron thermalization with superior coupling to neutron guides (Section 6.2.1.3.5) (Ageron, 1989; Lillie & Alsmiller, 1990; Alsmiller & Lillie, 1992).

6.2.1.3. *Beamline components*

Until recently, instrument design has been largely based on experience; however, in many cases, it is now possible to formulate a comprehensive description of the instrument and explore the impact of various parameters on instrument performance using an extensive array of computational methods (Johnson & Stephanou, 1978; Sivia *et al.*, 1990; Hjelm, 1996). In practice, it is the instrument design that provides access to the fundamental scattering processes, as briefly outlined in the following.

If a neutron specified by a wavevector $\mathbf{k}_1$ is incident on a sample with a scattering function $S(\mathbf{Q},\omega)$, all neutron scattering can be reduced to the simple form

$$\frac{\mathrm{d}^2\sigma}{\mathrm{d}\Omega\ \mathrm{d}E} = AS(\mathbf{Q},\omega),$$

where A is a constant containing experimental information, including instrumental resolution effects. The basic quantity to be measured is the partial differential cross section, which gives the fraction of neutrons of incident energy E scattered into an element

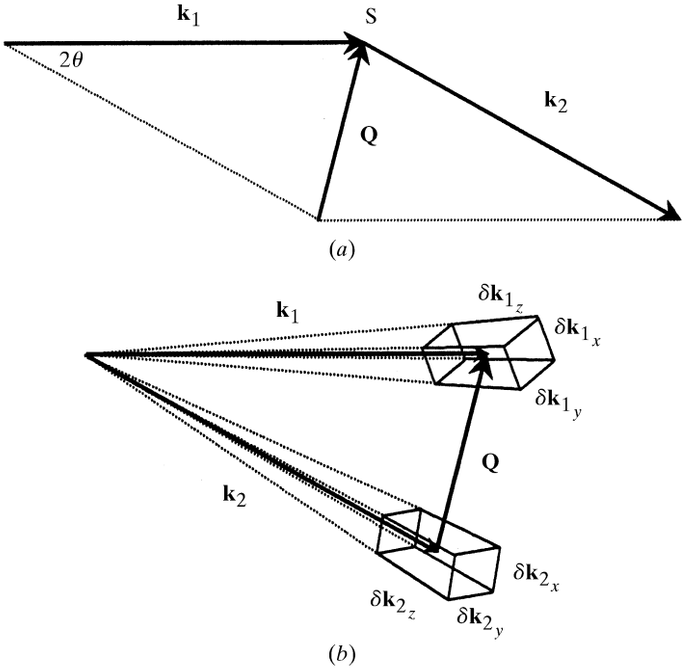

Fig. 6.2.1.3. (*a*) Schematic vector diagram for an elastic neutron-scattering event. A neutron, $\mathbf{k}_1$, is incident on a sample, S, and a scattered neutron, $\mathbf{k}_2$, is observed at an angle 2θ leading to a momentum transfer, $\mathbf{Q}$. (*b*) Schematic of an elastic neutron-scattering event illustrating the consequences of uncertainty in defining the incident neutron, $\mathbf{k}_1$, and determining the scattered neutron, $\mathbf{k}_2$. The volumes ($\delta\mathbf{k}_{1_x}$, $\delta\mathbf{k}_{1_y}$, $\delta\mathbf{k}_{1_z}$) and ($\delta\mathbf{k}_{2_x}$, $\delta\mathbf{k}_{2_y}$, $\delta\mathbf{k}_{2_z}$) constitute the instrument resolution function.

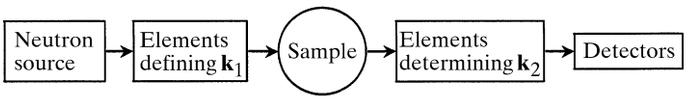

Fig. 6.2.1.4. A generic neutron-scattering instrument illustrating the classes of facilities and operators important to instrument design and assessment. Each class should be optimized and integrated into the overall instrument description.

of solid angle Ω with an energy between E' and $E' + \mathrm{d}E'$. The momentum transfer, $\mathbf{Q}$, is given in Fig. 6.2.1.3(*a*). The primary aim of a neutron-scattering experiment is to measure $\mathbf{k}_2$ to a predetermined precision (Bacon, 1962; Sears, 1989) (Fig. 6.2.1.3*b*). A generic neutron-scattering instrument used to achieve this aim is illustrated in Fig. 6.2.1.4. The instrument resolution function will be determined by uncertainties in $\mathbf{k}_1$ and $\mathbf{k}_2$, which are a direct consequence of (i) measures to increase the neutron flux at the sample position (to maximize wavelength spread, beam divergence, monochromator mosaic, for example) and (ii) uncertainties in geometric parameters (flight-path lengths, detector volume *etc*.).

6.2.1.3.1. *Collimators and filters*

In general, neutron-beam applications are flux-limited, and a major advantage will be realized by adopting advanced techniques in flux utilization. A reactor neutron source is large, and stochastic processes dominate the generation, moderation and general transport mechanisms. Because of radiation shielding, background reduction and space requirements for scattering instruments, reactor beam tubes have a minimum length of 3–4 m and cannot exceed a diameter of about 30 cm. The useful flux at the beam-tube exit is thus between 10^{-5} and 10^{-6} times the isotropic flux at its entry.

The most important aspect of beam-tube design, other than the size, is the position and orientation of the tube with respect to the reactor core. The widespread utilization of D_2O reflectors enables significant gains to be obtained from tangential tubes with maximal thermal neutron flux, and minimal fast neutron and γ fluxes. A similar result is accomplished in a split-core design by orienting the beam tubes toward the unfuelled region of the reactor core (Prask *et al.*, 1993).

There are two major groups of neutron-scattering instruments: those located close to and those located some distance from the neutron source. The first group is located to minimize the impact of the inverse square law on the neutron flux, and the second group is located to reduce background and provide more instrument space. In both cases, the first beamline component is a collimator to extract a neutron beam of divergence α from the reactor environment. The collimator is usually a beam tube of suitable dimensions for fully illuminating the wavelength-selection device. The angular acceptance of a collimator is determined strictly by the line-of-sight geometry between the source and the monochromator. Some geometric focusing may be appropriate, and a Soller collimator may be used to reduce α without reducing the beam dimensions. For technical reasons, the primary collimator is essentially fixed in dimensions and secondary collimators of adjustable dimensions may be required in more accessible regions outside the reactor shielding.

Neutron-beam filters are required for two main reasons: (i) to reduce beam contamination by fast neutron and γ radiation and (ii) to reduce higher- or lower-order harmonics from a monochromatic beam. Numerous single-crystal, polycrystalline and multilayer materials with suitable characteristics for filter applications are available (*e.g.* Freund & Dolling, 1995).

6.2.1.3.2. *Crystal monochromators*

The equilibrium neutron-wavelength distribution (Fig. 6.2.1.2) is a broad continuous distribution, and in most experiments it is necessary to select a narrow band in order to define $\mathbf{k}_1$. Neutron-wavelength selection can be achieved by Bragg scattering using single crystals to give well defined wavelengths; by polycrystalline material to remove a range of wavelengths; by a mechanical velocity selector; or by time-of-flight methods. The method chosen will depend on experimental requirements for the wavelength, λ, and wavelength spread, $\Delta\lambda/\lambda$.

Neutrons incident on a perfect single crystal of given interplanar spacing d will be diffracted to give specific wavelengths at angle 2θ according to the Bragg relation. A neutron beam, α_1, incident on a single crystal of mosaicity β will provide

$$\Delta\lambda/\lambda = [(\cot\theta \cdot \theta)^2 + (\Delta d/d)^2]^{1/2},$$

where

$$(\Delta\theta)^2 = \frac{\alpha_1^2\alpha_2^2 + \beta^2(\alpha_1^2 + \alpha_2^2)}{\alpha_1^2 + \alpha_2^2 + 4\beta^2}$$

and α_2 is the divergence of the (unfocused) diffracted beam.

Crystals for neutron monochromators must not only have a suitable d, but also high reflectivity and adequate β. Under these conditions, neutron beams with a $\Delta\lambda/\lambda$ of a few per cent are obtained. Typical crystals are Ge, Si, Cu and pyrolytic graphite. In order to increase the neutron flux at the sample, a number of mechanisms have been developed. These include focusing monochromatic crystals, frequently using Si or Ge (Riste, 1970; Mikula *et al.*, 1990; Copley, 1991; Magerl & Wagner, 1994; Popovici & Yelon, 1995), as well as stacked composite wafer monochromators (Vogt *et al.*, 1994; Schefer *et al.*, 1996).

One limitation of the use of crystal monochromators is the absence of suitable materials with large d. Indeed, the longest useable λ diffracted from pyrolytic graphite or Si is $\sim$5–6 Å.

6.2.1.3.3. *Multilayer monochromators and supermirrors*

Multilayers are especially useful for preparing a long-wavelength neutron beam from a cold source and for small-angle scattering experiments in which $\Delta\lambda/\lambda$ of about 0.1 is acceptable (Schneider & Schoenborn, 1984). Multilayer monochromators are essentially one-dimensional crystals composed of alternating layers of neutron-different materials (*e.g.* Ni and Ti) deposited on a substrate of low surface roughness. In order to produce multilayers of excellent performance, uniform layers are required with low interface roughness, low interdiffusion between layers and high scattering contrast. Various modifications (*e.g.* carbonation, partial hydrogenation) to the pure Ni and Ti bilayers improve the performance significantly by fine tuning the layer uniformity and contrast (Mâaza *et al.*, 1993). The minimum practical d-spacing is $\sim$50 Å and a useful upper limit is $\sim$150 Å. Multilayer monochromators have high neutron reflectivity ($>$0.95 is achievable), and their angular acceptance and bandwidth can be selected to produce a neutron beam of desired characteristics (Saxena & Schoenborn, 1977, 1988; Ebisawa *et al.*, 1979; Sears, 1983; Schoenborn, 1992*a*).

The supermirror, a development of the multilayer monochromator concept, consists of a precise number of layers with graded d-spacing. Such a device enables the simultaneous satisfaction of the Bragg condition for a range of λ and, hence, the transmission of a broader bandwidth (Saxena & Schoenborn, 1988; Hayter & Mook, 1989; Böni, 1997).

Polarizing multilayers and supermirrors (Schärpf & Anderson, 1994) facilitate valuable experimental opportunities, such as nuclear spin contrast variation (Stuhrmann & Nierhaus, 1996) and polarized neutron reflectometry (Majkrzak, 1991; Krueger *et al.*,

1996). Supermirrors consisting of Co and Ti bilayers display high contrast for neutrons with a magnetic moment parallel to the saturation magnetization and very low contrast for the remainder. With suitable modification of the substrate to absorb the antiparallel neutrons, a polarizing supermirror will produce a polarized neutron beam (polarization $> 90\%$) by reflection.

6.2.1.3.4. *Velocity selectors*

The relatively low speed of longer-wavelength neutrons ($\sim$600 m s^{-1} at 6 Å) enables wavelength selection by mechanical means (Lowde, 1960). In general, there are two classes of mechanical velocity selectors (Clark *et al.*, 1966). Rotating a group of short, parallel, curved collimators about an axis perpendicular to the beam direction will produce a pulsed neutron beam with λ and $\Delta\lambda/\lambda$ determined by the speed of rotation. This is a Fermi chopper. An alternate method is to translate short, parallel, curved collimators rapidly across the neutron beam, permitting only neutrons with the correct trajectory to be transmitted. This is achieved in the helical velocity selector, where the neutron wavelength is selected by the speed of rotation and $\Delta\lambda/\lambda$ can be modified by changing the angle between the neutron beam and the axis of rotation (Komura *et al.*, 1983). The neutron beam is essentially continuous, the resolution function is approximately triangular and the overall neutron transmission efficiency exceeds 75% in modern designs (Wagner *et al.*, 1992).

6.2.1.3.5. *Neutron guides*

In order for a collimator to be effective, its walls must absorb all incident neutrons. The angular acceptance is strictly determined by the line-of-sight geometry. Neutron guides can be used to improve this acceptance dramatically and to transport neutrons with a given angular distribution, almost without intensity loss, to regions distant from the source (Maier-Leibnitz & Springer, 1963). The basic principle of a guide is total internal reflection. This occurs for scattering angles less than the critical angle, θ_c, given by

$$\theta_c = 2(1 - n)^{1/2},$$

where n is the (neutron) index of refraction related to the coherent scattering length, b, of the wall material, *viz*,

$$n = 1 - (\lambda^2 \rho b/2\pi),$$

where ρ is the atom number density (in cm^{-3}). Among common materials, Ni with $b = 1.03 \times 10^{-12}$ cm, in combination with suitable physico-chemical properties, provides the best option, with a critical angle $\theta_c = 0.1\lambda$ (in Å). The dependence of θ_c on λ implies that guides are more effective for long-wavelength neutrons. With the introduction of supermirror guides with up to four times the θ_c of bulk Ni, both thermal and cold neutron beams are being transported and focused with high efficiency (Böni, 1997).

While a straight guide transports long wavelengths efficiently, it continues to transport all neutrons within the critical angle, including non-thermal neutrons emitted within the solid angle of the guide. This situation may be modified significantly by introducing a curvature to the guide. Since a curved neutron guide provides a form of spectral tailoring (cutoff or bandpass filters), simulation is a distinct advantage in exploring the impact of guide geometry on neutron-beam quality (van Well *et al.*, 1991; Copley & Mildner, 1992; Mildner & Hammouda, 1992).

6.2.1.4. *Detectors*

The detection of thermal neutrons is a nuclear event involving one of only a few nuclei with a sufficiently large absorption cross section (^{3}He, ^{10}B, ^{6}Li, Gd and ^{235}U). The secondary products (fragments, charged particles or photons) from the primary nuclear event are used to determine the location. Depending on the geometry of the instrument, either a spatially integrating or a position-sensitive detector is required (Convert & Forsyth, 1983; Crawford, 1992; Rausch *et al.*, 1992). The relatively weak neutron source is driving instrument design towards maximizing the number of neutrons collected per unit time, and, in many cases, this leads to the use of multiwire or position-sensitive detectors. The main performance characteristics for detector systems are position resolution, number of resolution elements, efficiency, parallax, maximum count rate, dynamic range, sensitivity to γ background and long-term stability.

6.2.1.4.1. *Multiwire proportional counters*

The principles of a multiwire proportional counter (MWPC) are well established (Sauli, 1977) and have wide application. For thermal neutron detection (Radeka *et al.*, 1996), the reaction of choice is

$$^3\mathrm{He} + \mathrm{n} \rightarrow {}^3\mathrm{H} + \mathrm{p} + 764\ \mathrm{keV}.$$

The 191 keV triton and the 573 keV proton are emitted in opposite directions and create a charge cloud whose dimensions are determined primarily by the pressure of a stopping gas. Depending on the work function of the gas mixture, approximately 3×10^4 electron–ion pairs are created. Low-noise gas amplification of this charge cloud occurs in an intense electric field created in the vicinity of the small diameter (20–30 µm) anode wires (Radeka, 1988). Typical gas gains of $\sim$10–50 lead to a total charge on the anode of $\sim$50–100 fC. The efficiency of the detector is determined by the pressure of ^{3}He, and the spatial resolution and count-rate capability are determined by the detector geometry and readout system. The event decoding is selected from the time difference (Borkowski & Kopp, 1975), charge division (Alberi *et al.*, 1975), centroid-finding filter (Radeka & Boie, 1980), or wire-by-wire techniques (Jacobé *et al.*, 1983; Knott *et al.*, 1997). Present MWPC technology offers opportunities and challenges to design a detector system that is totally integrated into the instrument design and optimizes data collection rate and accuracy (Schoenborn *et al.*, 1985, 1986; Schoenborn, 1992*b*).

A concept related to the MWPC is the micro-strip gas chamber (MSGC). With the MSGC, the general principles of gas detection and amplification apply; however, the anode is deposited on a suitable substrate (Oed, 1988, 1995; Vellettaz *et al.*, 1997). The MSGC can potentially improve the performance of the MWPC in some applications, particularly with respect to spatial resolution and count-rate capability.

6.2.1.4.2. *Image plates*

The principles underlying the operation of an image plate (IP) are presented in detail in Chapter 7.2. Briefly, the important difference between an IP for X-ray and neutron detection is the presence of a converter (either Gd_2O_3 or ^{6}Li). The role of the converter is to capture an incoming neutron and create an event within the IP that mimics the detection of an X-ray photon. For example, neutron capture in Gd produces conversion electrons that exit the Gd_2O_3 grains, enter neighbouring photostimulated luminescence (PSL) material and create colour centres to form a latent image (Niimura *et al.*, 1994; Takahashi *et al.*, 1996). A neutron IP may have a virtually unlimited area and a shape limited only by the requirement to locate the detection event in a suitable coordinate system. With a neutron-detection efficiency of up to 80% at $\sim$1–2 Å, a dynamic quantum efficiency of $\sim$25–30% can be obtained. The dynamic

range is intrinsically 1:10^5. The spatial resolution is primarily limited by scattering processes of the readout laser beam, and measured line spread functions are typically 150–200 μm. The γ sensitivity is high and may restrict the application to instruments with low ambient γ background.

Neutron IPs are integrating devices well suited to data-acquisition techniques with long accumulation times, such as Laue diffraction (Niimura *et al.*, 1997) and small-angle scattering. On-line readout is a distinct advantage (Cipriani *et al.*, 1997).

6.2.1.5. *Instrument resolution functions*

For accurate data collection, the instrument smearing contribution to the data must be known with some certainty, particularly when data are collected over an extended range with multiple instrument settings. A balance must be struck between instrument smearing and neutron flux at the sample position; however, careful instrument design can produce: (i) a good signal-to-background ratio, thereby partially offsetting the flux limitation, and (ii) facilities and procedures for determining the instrument resolution function (Johnson, 1986).

As an example, instrumental resolution effects in the small-angle neutron scattering (SANS) technique have been investigated in some detail. A 'typical' SANS instrument is located on a cold neutron source with an extended (and often variable) collimation system. The sample is as large as possible and the detector is large with low spatial resolution. The instrument is best described by pinhole geometry. Three major contributions to the smearing of an ideal curve are: (i) the finite λ, (ii) $\Delta\lambda/\lambda$ of the beam and (iii) the finite resolution of the detector. Indirect Fourier transform, Monte Carlo and analytical methods have been developed to analyse experimental data and predict the performance of a given combination of resolution-dependent elements (*e.g.* Wignall *et al.*, 1988; Pedersen *et al.*, 1990; Harris *et al.*, 1995).

6.2.2. Spallation neutron sources

Another phenomenon, quite different from the fission process (Section 6.2.1), that will produce neutrons uses high-energy particles to interact with elements of medium to high mass numbers. This process, called spallation, was first demonstrated by Seaborg and Perlman, who showed that the bombardment of nuclei by high-energy particles results in the emission of various nucleons. The nuclear processes involved in spallation (Prael, 1994) are complex and are summarized in Fig. 6.2.2.1. These processes have been investigated in some detail, and excellent background information is available (Hughes, 1988; Carpenter, 1977; Windsor, 1981). Present-day spallation sources typically use high-energy protons from an accelerator to bombard a heavy-metal target, such as W or U, and come in two types, using either a pulsed proton beam (*e.g.* ISIS or LANSCE) or a 'continuous' proton beam (SINQ).

The high-energy neutrons produced by spallation are moderated in a reflector region to intermediate energies and then reduced to thermal energies in a hydrogenous medium called the moderator (Russell *et al.*, 1996). These thermal neutrons are then extracted *via* beam pipes. A typical layout of a target system with reflectors and moderators is shown in Fig. 6.2.2.2.

The neutrons produced by the proton pulse travel along beam pipes as a function of their velocity, proportional to their energy. At a given distance from the target, neutrons of different energies are observed to arrive as a function of time, with the short-wavelength neutrons arriving first, followed by the longer-wavelength neutrons. Diffraction experiments are therefore carried out with pulsed 'polychromatic' neutron beams as a function of time; a time-resolved Laue pattern results. Clearly, the energy resolution of these beams depends on the volume of the neutron source. To achieve high energy resolution, the volume from which thermal neutrons are extracted is limited to the moderator by suitable use of liners and poisons (Fig. 6.2.2.2) that prevent thermal neutrons produced in the reflector from streaming into the beam pipe (decoupled moderators). The use of liners and poisons achieves high energy resolution, but at the expense of flux. The omission or reconfiguration of liners and poisons allows higher flux, but results in lower energy (wavelength) resolution (see Section 6.2.2.2).

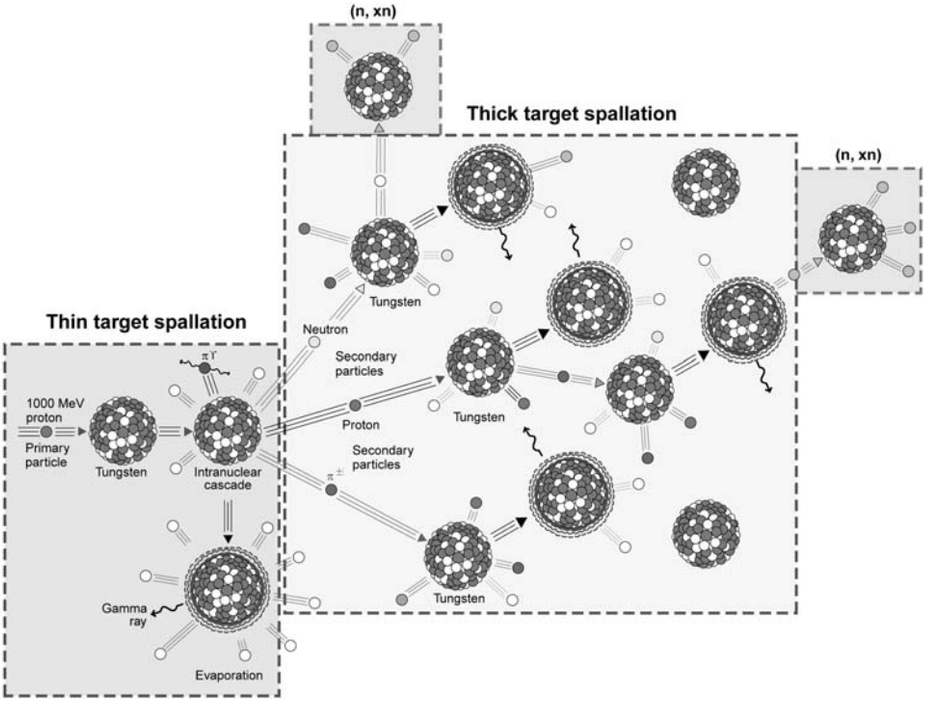

Fig. 6.2.2.1. Schematic presentation of the various nuclear processes encountered in spallation. The numerical analysis of these processes is carried out by two Monte Carlo-based codes – the *LAHET* code models the higher-energy nuclear interactions, while the *HMCNP* code models the thermal interactions and the transport of neutrons to the sample.

6.2.2.1. *Spallation neutron production*

Pulsed spallation neutrons are produced by protons generated by a particle accelerator (linac) with a frequency typically in the range 10 to 120 Hz. The proton pulses are often shaped in compressor rings to shorten the pulses from the millisecond range to less than a microsecond in duration, with currents reaching the sub-milliampere range at energies of 800 MeV or higher. The planned new spallation source at the Oak Ridge National Laboratory will have a proton energy of 1.2 GeV with a power of 1 MW and a repetition frequency of 60 Hz. The high-energy

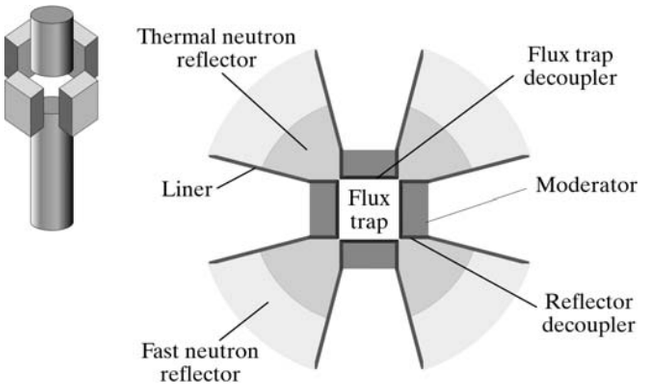

Fig. 6.2.2.2. Schematic diagram of a spallation target module depicting the inner Be and outer Pb reflector. Moderators are positioned close to the flux trap, which is between the upper and lower tungsten targets. This schematic includes the location of the various decoupling agents (Cd) for fully decoupled moderators. For the partially coupled moderator system being fabricated for a protein-crystallography station at Los Alamos, the depicted decouplers affecting the given moderator are removed and replaced by a single decoupling layer placed between the outer Pb and the inner Be reflector. This can be done with a split-target arrangement that utilizes a two-tiered moderator system, permitting coupled moderators to be on one tier and decoupled moderators on the other.

protons hit a cooled target (typically W or U) and produce high- and medium-energy neutrons in equivalent bursts. The fast neutrons are moderated in the surrounding reflector and returned to the moderator (Fig. 6.2.2.2). In addition to direct collision interactions, the high-energy neutrons also produce low-energy neutrons *via* (n, *x*n) reactions in the Pb and Be reflectors. Final moderation to the thermal energies used for diffraction experiments is completed *via* interactions with light elements, such as H_2O or liquid H_2, in the moderator module.

6.2.2.2. *Moderators*

Moderators for pulsed spallation neutron sources are nearly always composed of hydrogenous material of about 1 l in volume. Either a thermal or fast reflector surrounds the moderator. Reflectors composed of materials with strong neutron slowing-down properties, such as Be or D_2O, are called thermal reflectors; fast reflectors are composed of materials with weaker slowing-down powers, such as Pb or Ni. In order to retain a narrow pulse width in time, thermal neutrons produced in the reflector region are prevented from reaching the moderator module by judicious use of liners and poisons (typically Cd or Gd) that allow transmission of fast (high and intermediate energy) neutrons, but are opaque to thermal neutrons. Such a moderator arrangement is said to be decoupled, and all thermal neutrons extracted by the beam pipe originate in the moderator itself. For a 0.25 μs-long proton pulse, the target (W or U) produces a fast neutron burst of about 0.5 μs in duration. These very high energy neutrons are slowed down in the reflector and are reflected back into the moderator to produce a thermal neutron pulse of about 1 μs duration. Since thermal neutrons produced in the reflector are prevented from reaching the moderator by the use of liners and poisons, the experiment sees only thermal neutrons originating in the moderator.

By moving the decoupling and poison layers away from the moderator and into the reflector, one can redefine how actively a reflector communicates *via* neutrons with a moderator and how some of the thermal neutrons produced in the reflector are extracted (Schoenborn *et al.*, 1999). The result is an increase in flux, both peak- and time-integrated, but at the expense of the sharply defined

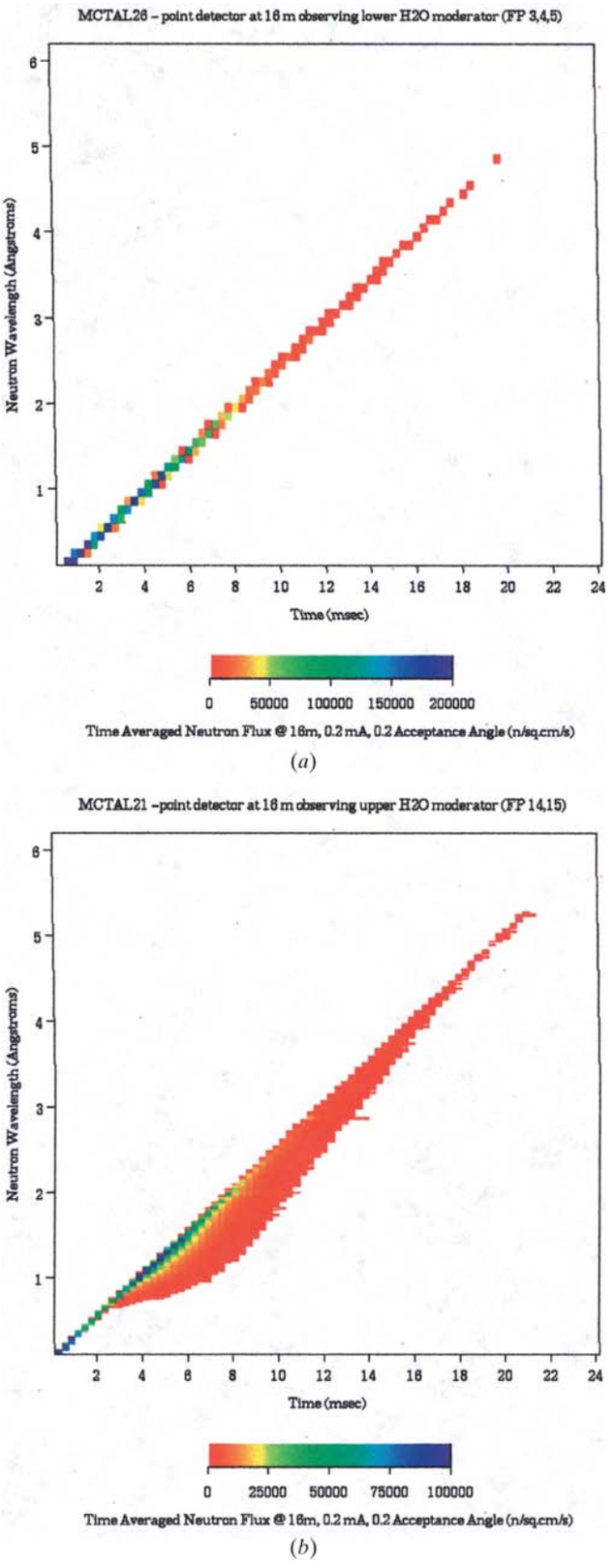

Fig. 6.2.2.3. Neutron flux given as a time–wavelength spectrum for (*a*) a fully decoupled system and (*b*) for a fully coupled system. Both spectra are based on Monte Carlo codes (*LAHET* and *HMCNP*) and are calculated for a target-to-sample distance of 10 m. Comparison of such Monte Carlo results calculated using the geometry of an existing beamline shows agreement with measured values to within 10%.

time distribution. With the elimination of all liners and poisons, a fully coupled system is obtained with a flux gain of about 6 × but with poorer wavelength resolution. The wavelength distribution at a given distance from the moderator is shown in Fig. 6.2.2.3(*a*) for the fully decoupled case and in Fig. 6.2.2.3(*b*) for the fully coupled case. For a decoupled moderator, the slowing-down power of the reflector is not as critical as it is for the coupled one. In the coupled moderator, it is beneficial to use a thermal reflector in the volume immediately surrounding the moderator because this enhances the peak thermal neutron flux. The decay constant of the neutron pulse can be tailored to match the diffractometer resolution by using a composite reflector composed of an inner thermal reflector and an outer fast reflector. The outer reflector can have a moderate thermal neutron absorption cross section, or the inner reflector can be decoupled from the outer reflector in the same manner that a moderator is decoupled from a reflector. The decay constant can then be varied by simply adjusting the size of the inner reflector (Russell *et al.*, 1996). The wavelength or energy distribution of thermal neutrons produced in the moderator is dependent on the temperature of the moderating medium, as described in Section 6.2.1.2.

For neutron protein crystallography, a moderator with an intermediate temperature between a cold and thermal moderator would be most appropriate. This can be achieved with a composite moderator composed of a thermal and a cold moderator in a symbiotic configuration, or a cold methane system.

6.2.2.3. *Beamline optics*

A chosen wavelength band (say, 1 to 6 Å) is selected by the use of rotating disks (called choppers) composed of neutron absorbing and transparent material. These choppers are synchronized to the proton pulse. The T0 chopper can open the beam a short time after the impact of the proton pulse and stop the high- and intermediate-energy radiation from reaching the sample and the detector. The T1 chopper can select the long-wavelength edge and prevent frame overlap. Since the T0 chopper is designed to stop the initial γ and high-energy neutron radiation, it is usually made of thick (30 cm) blades of Ni, while the T1 chopper is simpler in construction since it is designed to stop only thermal neutrons.

The flight-path lengths of relevant spallation neutron instruments are quite long; the Los Alamos Spallation Neutron Source has a 28 m path length for its protein crystallography station on a partially decoupled moderator. For a fully decoupled system, a flight-path length of 10 m would provide adequate energy resolution.

For protein crystallography, a beam divergence matched to the mosaicity of the crystal provides the best peak-to-background ratio. For such cases, a beam divergence of $\pm 0.1^\circ$ can be achieved using circular collimating disks of Boral or Boron-Poly to form a cone that views most of the moderator (typically 12×12 cm) and channels the neutron beam onto the detector with a final aperture of millimetre dimensions. Another approach uses focusing mirrors, and calculations show that toroidal geometry will produce a gain in intensity of 1.5 to 2 times, depending on flight distance and beam divergence (Schoenborn, 1992*a*).

6.2.2.4. *Time-of-flight techniques*

Because of the time structure inherent at a spallation source, diffraction experiments are carried out as a function of time and use a large part of the neutron energy spectrum. For protein crystallography, this wavelength range might cover from 1 to 5 Å, depending on the unit-cell size and the moderator used. This is particularly advantageous and allows the collection of data in a quasi-Laue fashion (Schoenborn, 1992*a*) without the drawback of spot overlap normally encountered in Laue patterns. Data are collected in a stroboscopic fashion, synchronized to the pulsed nature of the source, with each separately recorded time frame producing a Laue pattern from a narrow, gradually increasing wavelength band. The summation of all time frames will produce a true Laue pattern. The collection and analysis of these quasi-Laue patterns (time frames) will eliminate spot overlap and yield a greatly improved peak-to-background ratio, since the integrated background is produced only by the small wavelength band responsible for a particular diffraction peak.

6.2.2.5. *Data-collection considerations*

Single-event-counting multiwire chambers with centroid-finding electronics (introduced in Section 6.2.1.4) are well suited for the type of time-sliced data collection that is mandatory for spallation neutron instruments. For large, high-resolution, multi-segmented detectors collecting about 100 time slices per cycle, data memories in the order of 100 million pixels are required. The number of time slices that needs to be collected to produce the optimum peak-to-background ratio depends on the characteristics (wavelength bandwidth) of the coupled or decoupled moderator.

Data-integration techniques are similar to those for the classic reactor case (Section 6.2.1.5), but contain a time (wavelength) dimension and no crystal stepping. The crystal is stationary and the reflection is 'scanned' as a function of time by the wavelength band. Time-dependent reflection overlap, caused by long pulse decay (particularly observed in fully coupled moderators), can be a problem. Such overlaps can be minimized by using a partially coupled moderator (Schoenborn *et al.*, 1999).

6.2.3. Summary

In the preceding sections, a brief overview has been presented of (i) the two main types of neutron sources and (ii) some of the primary components required to prepare a neutron beam for a neutron-scattering instrument. It has been assumed that as well as macromolecular crystallography, membrane and fibre diffraction, small-angle neutron scattering (see Chapter 19.4) is of interest. From a structural-biology user perspective, the advantages and disadvantages of reactor-based and spallation-source-based facilities are difficult to assess, since only very limited use of spallation sources has been documented. Direct comparisons between the performances of neutron-scattering instruments and sources are difficult, and would undoubtedly change as facilities are progressively upgraded (Carpenter & Yelon, 1986; Richter & Springer, 1998). Calculations show, however, that the use of time-of-flight techniques with partially coupled moderators on a spallation neutron source is ideal for structural-biology diffraction studies and promises to yield an effective gain of an order of magnitude in intensity (Schoenborn, 1996). When the protein crystallographic diffraction instrument now being built at LANSCE is completed in 2000, a more meaningful comparison will be possible between a premier spallation-source-based instrument and comparable reactor-based instruments.

In summary, the neutron source plays a pivotal role in the design and utility of an experiment in macromolecular crystallography, membrane and fibre diffraction, and small-angle neutron scattering. However, innovative design of the scattering instrument using the latest technology (*e.g.* image plates or large MWPCs) can partially offset certain negative impacts of the source and make an enormous difference to the instrument as a user facility. In general, neutron sources are national or regional facilities and consequently carry special requirements for user access. Therefore, a local, well equipped, medium-flux neutron source may be more suitable to test potential experiments and the premier international facility should be used only where required.

References

6.1

Arndt, U. W., Duncumb, P., Long, J. V. P., Pina, L. & Inneman, A. (1998). *Focusing mirrors for use with microfocus X-ray tubes. J. Appl. Cryst.* **31**, 733.

Arndt, U. W., Long, J. V. P. & Duncumb, P. (1998). *A microfocus X-ray tube used with focusing collimators. J. Appl. Cryst.* **31**, 936–944.

Arndt, U. W. & Stubbings, S. J. (1988). *Miniature ionisation chambers. J. Appl. Cryst.* **21**, 577.

Bailey, R. L. (1978). *The design and operation of magnetic liquid shaft seals.* In *Thermomechanics of magnetic fluids*, edited by B. Berkovsky. London: Hemisphere.

Beuville, E., Beche, J.-F., Cork, C., Douence, V., Earnest, J., Millaud, D., Nygren, H., Padmore, B., Turko, G., Zizka, G., Datte, P. & Xuong Ng, H. (1997). *Two-dimensional pixel array sensor for protein crystallography. Proc. SPIE*, **2859**, 85–92.

Bilderback, D. H., Thiel, D. J., Pahl, R. & Brister, K. E. (1994). *X-ray applications with glass-capillary optics. J. Synchrotron Rad.* **1**, 37–42.

Bly, P. & Gibson, D. (1996). *Polycapillary optics focus and collimate X-rays. Laser Focus World*, March issue.

Buras, B. & Tazzari, S. (1984). Editors. *European Synchrotron Radiation Facility.* Geneva: ESRP.

Elliott, A. (1965). *The use of toroidal reflecting surfaces in X-ray diffraction cameras. J. Sci. Instrum.* **42**, 312–316.

Forsyth, J. M. & Frankel, R. D. (1984). *Experimental facility for nanosecond time-resolved low-angle X-ray diffraction experiments using a laser-produced plasma source. Rev. Sci. Instrum.* **55**, 1235–1242.

Fourme, R., Ducruix, A., Ries-Kautt, M. & Capelle, B. (1995). *The perfection of protein crystals probed by direct recording of Bragg reflection profiles with a quasi-planar X-ray wave. J. Synchrotron Rad.* **2**, 136–142.

Franks, A. (1995). *An optically focusing X-ray diffraction camera. Proc. Phys. Soc. London Sect. B*, **68**, 1054–1069.

Genz, H., Graf, H.-D., Hoffmann, P., Lotz, W., Nething, U., Richter, A., Kohl, H., Weickenmeyer, A., Knüpfer, W. & Sellschop, J. P. F. (1990). *High intensity electron channeling and perspectives for a bright tunable X-ray source. Appl. Phys. Lett.* **57**, 2956–2958.

Green, M. (1963). *The target absorption correction in X-ray microanalysis.* In *X-ray optics and X-ray microanalysis*, edited by H. H. Pattee, V. E. Cosslett & A. Engström, pp. 361–377. New York and London: Academic Press.

Green, M. & Cosslett, V. E. (1968). *Measurements of K, L and M shell X-ray production efficiencies. Br. J. Appl. Phys. Ser.* 2, **1**, 425–436.

Hofmann, A. (1978). *Quasi-monochromatic synchrotron radiation from undulators. Nucl. Instrum. Methods*, **152**, 17–21.

International Tables for Crystallography (1999). Vol. C. *Mathematical, physical and chemical tables*, edited by A. J. C. Wilson & E. Prince. Dordrecht: Kluwer Academic Publishers.

Ishimura, T., Shiraiwa, Y. & Sawada, M. (1957). *The input power limit of the cylindrical rotating anode of an X-ray tube. J. Phys. Soc. Jpn*, **12**, 1064–1070.

Kirkpatrick, P. & Baez, A. V. (1948). *J. Opt. Soc. Am.* **56**, 1–13.

Kirz, J. (1974). *Phase zone plates for X-rays and the extreme UV. J. Opt. Soc. Am.* **64**, 301–309.

Kleffer, J. C., Chaker, M., Matte, J. P., Pépin, H., Côté, C. Y., Beaudouin, Y., Johnston, T. W., Chien, C. Y., Coe, S., Mourou, G. & Peyrusse, O. (1993). *Ultra-fast X-ray sources. Phys. Fluids*, **B5**, 2676–2681.

Kohra, K., Ando, M., Natsushita, T. & Hashizume, H. (1978). *Nucl. Instrum. Methods*, **152**, 161–166.

Kumakhov, M. A. & Komarov, F. K. (1990). *Phys. Rep.* **191**, 289–350.

Lemonnier, M., Fourme, R., Rousseaux, F. & Kahn, R. (1978). *X-ray curved-crystal monochromator system at the storage ring DCI. Nucl. Instrum. Methods*, **152**, 173–177.

MacDonald, C. A., Owens, S. M. & Gibson, W. M. (1999). *Polycapillary X-ray optics for microdiffraction. J. Appl. Cryst.* **32**, 160–167.

Milch, J. R. (1983). *A focusing X-ray camera for recording low-angle diffraction from small specimens. J. Appl. Cryst.* **16**, 198–203.

Montel, M. (1957). *X-ray microscopy with catamegonic roof mirrors.* In *X-ray microscopy and microradiography*, edited by V. E. Cosslett, A. Engstrom & H. H. Pattee Jr, pp. 177–185. New York: Academic Press.

Müller, A. (1929). *A spinning target X-ray generator and its input limit. Proc. R. Soc. London Ser. A*, **125**, 507–516.

Müller, A. (1931). *Further estimates of the input limits of X-ray generators. Proc. R. Soc. London Ser. A*, **132**, 646–649.

Nagel, D. J. (1980). *Comparison of X-ray sources. Ann. N. Y. Acad. Sci.* **342**, 235–247.

Nave, C., Clark, G., Gonzalez, A., McSweeney, S., Hart, M. & Cummings, S. (1995). *Tests of an asymmetric monochromator to provide increased flux on a synchrotron radiation beam line. J. Synchrotron Rad.* **2**, 292–295.

Oosterkamp, W. J. (1948). *The heat dissipation in the anode of an X-ray tube. Philips Res. Rep.* **3**, 49–59, 161–173, 303–317.

Osmic Inc. (1998). Sales literature. Osmic Inc., Troy, Michigan, USA.

Padmore, H. A., Ackermann, G., Celestre, R., Chang, C. H., Franck, K., Howells, M., Hussain, Z., Irick, S., Locklin, S., MacDowell, A. A., Patel, J. R., Rah, S. Y., Renner, T. R. & Sandler, R. (1997). *Submicron white-beam focusing using elliptically bent mirrors. Synchrotron Radiat. News*, **10**, 18–26.

Phillips, W. C. (1985). *X-ray sources. Methods Enzymol.* **114**, 300–316.

Piestrup, M. A., Boyers, D. G., Pincus, C. I., Harris, J. L., Maruyama, X. K., Bergstrom, J. C., Caplan, H. S., Silzer, R. M. & Skopik, D. M. (1991). *Quasimonochromatic X-ray source using photo-absorption-edge transition radiation. Phys. Rev. A*, **43**, 3653–3661.

Quintana, J. P. & Hart, M. (1995). *Adaptive silicon monochromators for high-power wigglers; design, finite-element analysis and laboratory tests. J. Synchrotron Rad.* **2**, 119–123.

Schuster, M. & Göbel, H. (1997). *Application of graded multi-layer optics in X-ray diffraction. Adv. X-ray Anal.* **39**, 57–71.

Schwinger, J. (1949). *On the classical radiation of accelerated electrons. Phys. Rev.* **75**, 1912–1925.

Silfhout, R. G. van (1998). *A new water-cooled monochromator at DORIS III. Synchrotron Radiat. News*, **11**, 11–13.

Smither, R. K. (1982). *New methods for focusing X-rays and gamma rays. Rev. Sci. Instrum.* **53**, 131–141.

Winick, H. (1980). *Properties of synchrotron radiation.* In *Synchrotron radiation research*, edited by H. Winick & S. Doniach. New York: Plenum.

Yoshimatsu, M. & Kozaki, S. (1977). *High brilliance X-ray source.* In *X-ray optics*, edited by H.-J. Queisser, ch. 2. Berlin: Springer.

6.2

Ageron, P. (1989). *Cold neutron sources at ILL. Nucl. Instrum. Methods A*, **284**, 197–199.

Akcasu, A. Z., Lellouche, G. S. & Shotkin, L. M. (1971). *Mathematical methods in nuclear reactor dynamics.* New York: Academic Press.

Alberi, J., Fischer, J., Radeka, V., Rogers, L. C. & Schoenborn, B. P. (1975). *A two-dimensional position-sensitive detector for thermal neutrons. Nucl. Instrum. Methods*, **127**, 507–523.

Alsmiller, R. G. & Lillie, R. A. (1992). *Design calculations for the ANS cold source. Part II. Heating rates. Nucl. Instrum. Methods A*, **321**, 265–270.

Bacon, G. E. (1962). *Neutron diffraction.* Oxford University Press.

Böni, P. (1997). *Supermirror-based beam devices. Physica B*, **234–236**, 1038–1043.

6.2 (*cont.*)

Borkowski, C. J. & Kopp, M. K. (1975). *Design and properties of position-sensitive proportional counters using resistance-capacitance position encoding. Rev. Sci. Instrum.* **46**, 951–962.

Carpenter, J. M. (1977). *Pulsed spallation neutron sources for slow neutron scattering. Nucl. Instrum. Methods*, **145**, 91–113.

Carpenter, J. M. & Yelon, W. B. (1986). *Neutron sources.* In *Methods of experimental physics*, Vol. 23A. New York: Academic Press.

Cipriani, F., Castagna, J.-C., Caustre, L., Wilkinson, C. & Lehmann, M. S. (1997). *Large area neutron and X-ray image-plate detectors for macromolecular biology. Nucl. Instrum. Methods A*, **392**, 471–474.

Clark, C. D., Mitchell, E. W. J., Palmer, D. W. & Wilson, I. H. (1966). *The design of a velocity selector for long wavelength neutrons. J. Sci. Instrum.* **43**, 1–5.

Convert, P. & Forsyth, J. B. (1983). Editors. *Position-sensitive detection of thermal neutrons.* London: Academic Press.

Copley, J. R. D. (1991). *Acceptance diagram analysis of the performance of vertically curved neutron monochromators. Nucl. Instrum. Methods*, **301**, 191–201.

Copley, J. R. D. & Mildner, D. F. R. (1992). *Simulation and analysis of the transmission properties of curved–straight neutron guide systems. Nucl. Sci. Eng.* **110**, 1–9.

Crawford, R. K. (1992). *Position-sensitive detection of slow neutrons – survey of fundamental principles. SPIE*, **1737**, 210–223.

Ebisawa, T., Achiwa, N., Yamada, S., Akiyoshi, T. & Okamoto, S. (1979). *Neutron reflectivities of Ni–Mn and Ni–Ti multilayers for monochromators and supermirrors. J. Nucl. Sci. Technol.* **16**, 647–659.

Freund, A. K. & Dolling, G. (1995). *Devices for neutron beam definition.* In *International tables for crystallography*, Vol. C. *Mathematical, physical and chemical tables*, edited by A. J. C. Wilson, pp. 375–382. Dordrecht: Kluwer Academic Publishers.

Glasstone, S. & Sesonske, A. (1994). *Nuclear reactor engineering.* New York: Chapman and Hall.

Hallsall, M. J. (1995). *WIMS – a general purpose code for reactor core analysis.* AEA Technology, Vienna.

Harris, P., Lebech, B. & Pedersen, J. S. (1995). *The three-dimensional resolution function for small-angle scattering and Laue geometries. J. Appl. Cryst.* **28**, 209–222.

Hayter, J. B. & Mook, H. A. (1989). *Discrete thin-film multilayer design for X-ray and neutron supermirrors. J. Appl. Cryst.* **22**, 35–41.

Hjelm, R. (1996). Editor. *Proceedings of the workshop on methods for neutron scattering instrumentation design.* Lawrence Berkeley National Laboratory, USA.

Hughes, H. G. III (1988). *Monte Carlo simulation of the LANSCE target geometry. Proceedings of the tenth international collaboration on advanced neutron sources*, p. 455. New York: Institute of Physics.

Jacobé, J., Feltin, D., Rambaud, A., Ratel, F., Gamon, M. & Pernock, J. B. (1983). *High pressure ^{3}He multielectrode detectors for neutron localisation.* In *Position-sensitive detection of thermal neutrons*, edited by P. Convert & J. B. Forsyth, pp. 106–119. London: Academic Press.

Jakeman, D. (1966). *Physics of nuclear reactors.* London: The English Universities Press.

Johnson, M. W. (1986). Editor. *Workshop on neutron scattering data analysis.* Rutherford Appleton Laboratory, Chilton, England. Bristol: Institute of Physics.

Johnson, M. W. & Stephanou, C. (1978). *MCLIB: a library of Monte Carlo subroutines for neutron scattering problems.* Report RL-78-090. Science Research Council, Chilton, England.

Knott, R. B., Smith, G. C., Watt, G. & Boldeman, J. B. (1997). *A large 2D PSD for thermal neutron detection. Nucl. Instrum. Methods A*, **392**, 62–67.

Komura, S., Takeda, T., Fujii, H., Toyoshima, Y., Osamura, K., Mochiki, K. & Hasegawa, K. (1983). *The 6-meter neutron small-angle scattering spectrometer at KUR. Jpn. J. Appl. Phys.* **22**, 351–356.

Kostorz, G. (1979). *Neutron scattering. Treatise on materials science and technology*, Vol. 15. New York: Academic Press.

Krueger, S., Koenig, B. W., Orts, W. J., Berk, N. F., Majkrzak, C. F. & Gawrisch, K. (1996). *Neutron reflectivity studies of single lipid bilayers supported on planar substrates.* In *Neutrons in biology*, edited by B. P. Schoenborn & R. B. Knott, pp. 205–213. New York: Plenum Press.

Lewis, E. E. & Miller, W. F. (1993). *Computational methods of neutron transport.* Washington: American Nuclear Society Inc.

Lillie, R. A. & Alsmiller, R. G. (1990). *Design calculations for the ANS cold neutron source. Nucl. Instrum. Methods A*, **295**, 147–154.

Lowde, R. D. (1960). *The principles of mechanical neutron-velocity selection. J. Nucl. Energy*, **11**, 69–80.

Mâaza, M., Farnoux, B., Samuel, F., Sella, C., Wehling, F., Bridou, F., Groos, M., Pardo, B. & Foulet, G. (1993). *Reduction of the interfacial diffusion in Ni–Ti neutron-optics multilayers by carburation of the Ni–Ti interfaces. J. Appl. Cryst.* **26**, 574–582.

Magerl, A. & Wagner, V. (1994). Editors. *Proceedings of the workshop on focusing Bragg optics. Nucl. Instrum. Methods A*, Vol. 338.

Maier-Leibnitz, H. & Springer, T. (1963). *The use of neutron optical devices on beam-hole experiments. J. Nucl. Energy*, **17**, 217–225.

Majkrzak, C. F. (1991). *Polarised neutron reflectometry. Physica B*, **173**, 75–88.

Mikula, P., Krüger, E., Scherm, R. & Wagner, V. (1990). *An elastically bent silicon crystal as a monochromator for thermal neutrons. J. Appl. Cryst.* **23**, 105–110.

Mildner, D. F. R. & Hammouda, B. (1992). *The transmission of curved neutron guides with non-perfect reflectivity. J. Appl. Cryst.* **25**, 39–45.

Niimura, N., Karasawa, Y., Tanaka, I., Miyahara, J., Takahashi, K., Saito, H., Koizumi, S. & Hidaka, M. (1994). *An imaging plate neutron detector. Nucl. Instrum. Methods A*, **349**, 521–525.

Niimura, N., Minezaki, Y., Nonaka, T., Castagna, J.-C., Cipriani, F., Høghøj, P., Lehmann, M. S. & Wilkinson, C. (1997). *Neutron Laue diffractometry with an imaging plate provides an effective data collection regime for neutron protein crystallography. Nature Struct. Biol.* **4**, 909–914.

Oed, A. (1988). *Position-sensitive detector with microstrip anode for electron multiplication with gases. Nucl. Instrum. Methods A*, **263**, 351–359.

Oed, A. (1995). *Properties of micro-strip gas chambers (MSGC) and recent developments. Nucl. Instrum. Methods A*, **367**, 34–40.

Pedersen, J. S., Posselt, D. & Mortensen, K. (1990). *Analytical treatment of the resolution function for small-angle scattering. J. Appl. Cryst.* **23**, 321–333.

Popovici, M. & Yelon, W. B. (1995). *Focusing monochromators for neutron diffraction. J. Neutron Res.* **3**, 1–26.

Prael, R. E. (1994). *A review of the physics models in the LAHET code*. Report LA-UR-94-1817. Los Alamos National Laboratory, USA.

Prask, H. J., Rowe, J. M., Rush, J. J. & Schroeder, I. G. (1993). *The NIST cold neutron research facility. J. Res. NIST*, **98**, 1–14.

Pynn, R. (1984). *Neutron scattering instrumentation at reactor based installations. Rev. Sci. Instrum.* **55**, 837–848.

Radeka, V. (1988). *Low noise techniques in detectors. Annu. Rev. Nucl. Part. Sci.* **38**, 217–277.

Radeka, V. & Boie, R. A. (1980). *Centroid finding method for position-sensitive detectors. Nucl. Instrum. Methods*, **178**, 543–554.

Radeka, V., Schaknowski, N. A., Smith, G. C. & Yu, B. (1996). *High precision thermal neutron detectors.* In *Neutrons in biology*, edited by B. P. Schoenborn & R. B. Knott, pp. 57–67. New York: Plenum Press.

Rausch, C., Bücherl, T., Gähler, R., Seggern, H. & Winnacker, A. (1992). *Recent developments in neutron detection. SPIE*, **1737**, 255–263.

Richter, D. & Springer, T. (1998). *A twenty years forward look at neutron scattering facilities in the OECD countries and Russia*. OECD Publication. Strasbourg: European Science Foundation.

6.2 (*cont.*)

Riste, T. (1970). *Singly bent graphite monochromators for neutrons. Nucl. Instrum. Methods.* **86**, 1–4.

Russell, G. J., Ferguson, P. D., Pitcher, E. J. & Court, J. D. (1996). *Neutronics and the MLNSC spallation target system*. In *Applications of accelerators in research and industry – proceedings of the 14th international conference*, edited by J. L. Duggan and I. L. Morgan. AIP Conference Proceedings, Vol. 392, pp. 361–364.

Sauli, F. (1977). *Principles of operation of multiwire proportional and drift chambers.* Report CERN-77-09. CERN, Geneva, Switzerland.

Saxena, A. M. & Schoenborn, B. P. (1977). *Multilayer neutron monochromators. Acta Cryst.* A**33**, 805–813.

Saxena, A. M. & Schoenborn, B. P. (1988). *Multilayer monochromators for neutron spectrometers. Mater. Sci. Forum*, **27/28**, 313–318.

Schärpf, O. & Anderson, I. S. (1994). *The role of surfaces and interfaces in the behaviour of non-polarizing and polarizing supermirrors. Physica B*, **198**, 203–212.

Schefer, J., Medarde, M., Fischer, S., Thut, R., Koch, M., Fischer, P., Staub, U., Horisberger, M., Bottger, G. & Donni, A. (1996). *Sputtering method for improving neutron composite germanium monochromators. Nucl. Instrum. Methods A*, **372**, 229–232.

Schneider, D. K. & Schoenborn, B. P. (1984). *A new neutron small-angle diffraction instrument at the Brookhaven High Flux Beam Reactor.* In *Neutrons in biology*, edited by B. P. Schoenborn, pp. 119–141. New York: Plenum Press.

Schoenborn, B. P. (1992*a*). *Multilayer monochromators and super mirrors for neutron protein crystallography using a quasi Laue technique. SPIE*, **1738**, 192–199.

Schoenborn, B. P. (1992*b*). *Area detectors for neutron protein crystallography. SPIE*, **1737**, 235–243.

Schoenborn, B. P. (1996). *A protein crystallography station at the Los Alamos Neutron Science Center*. Report LA-UR-96-3508, 11–64. Los Alamos National Laboratory, USA.

Schoenborn, B. P., Court, D., Larson, A. C. & Ferguson, P. (1999). *Moderator decoupling options for structural biology at spallation neutron sources. J. Neutron Res.* **7**, 89–106.

Schoenborn, B. P., Saxena, A. M., Stamm, M., Dimmler, G. & Radeka, V. (1985). *A neutron spectrometer with a two-dimensional detector for time resolved studies. Aust. J. Phys.* **38**, 337–351.

Schoenborn, B. P., Schefer, J. & Schneider, D. (1986). *The use of wire chambers in structural biology. Nucl. Instrum. Methods A*, **252**, 180–187.

Sears, V. F. (1983). *Theory of multilayer neutron monochromators. Acta Cryst.* A**39**, 601–608.

Sears, V. F. (1989). *Neutron optics: an introduction to the theory of neutron optical phenomena and their applications. Oxford series on neutron scattering in condensed matter.* New York: Oxford University Press.

Sivia, D. S., Silver, R. N. & Pynn, R. (1990). *The Bayesian approach to optimal instrument design.* In *Neutron scattering data analysis*, edited by M. W. Johnson, Institute of Physics Conference Series, Vol. 107, pp. 45–55.

Soodak, H. (1962). Editor. *Reactor handbook.* New York: Wiley.

Spanier, J. & Gelbard, E. M. (1969). *Monte Carlo principles and neutron transport problems.* London: Addison-Wesley.

Stamm'ler, R. J. J. & Abbate, M. J. (1983). *Methods of steady-state reactor physics in nuclear design.* London: Academic Press.

Stuhrmann, H. B. & Nierhaus, K. H. (1996). *The determination of the in situ structure by nuclear spin contrast variation*. In *Neutrons in biology*, edited by B. P. Schoenborn & R. B. Knott, pp. 397–413. New York: Plenum Press.

Takahashi, K., Tazaki, S., Miyahara, J., Karasawa, Y. & Niimura, N. (1996). *Imaging performance of imaging plate neutron detectors. Nucl. Instrum. Methods A*, **377**, 119–122.

Vellettaz, N., Assaf, J. E. & Oed, A. (1997). *Two dimensional gaseous microstrip detector for thermal neutrons. Nucl. Instrum. Methods A*, **392**, 73–79.

Vogt, T., Passell, L., Cheung, S. & Axe, J. D. (1994). *Using wafer stacks as neutron monochromators. Nucl. Instrum. Methods A*, **338**, 71–77.

Wagner, V., Friedrich, H. & Wille, P. (1992). *Performance of a high-tech neutron velocity selector. Physica B*, **180–181**, 938–940.

Weisman, J. (1983). Editor. *Elements of nuclear reactor design*. Amsterdam: Elsevier Scientific Publishing Company.

Well, A. A. van, de Haan, V. O. & Mildner, D. F. R. (1991). *The average number of reflections in a curved neutron guide. Nucl. Instrum. Methods A*, **309**, 284–286.

West, C. D. (1989). *The US advanced neutron source*. ICANS X, Los Alamos USA, pp. 643–654.

Wignall, G. D., Christen, D. K. & Ramakrishnan, V. (1988). *Instrumental resolution effects in small-angle neutron scattering. J. Appl. Cryst.* **21**, 438–451.

Williams, M. M. R. (1966). *The slowing down and thermalization of neutrons*. Amsterdam: North Holland.

Windsor, C. G. (1981). *Pulsed neutron scattering*. London: Wiley.

Windsor, C. G. (1986). *Experimental techniques*. In *Methods of experimental physics*, Vol. 23A. New York, London: Academic Press.